A NEW 3-D ELECTROMAGNETIC SOLVER FOR THE DESIGN OF ARBITRARILY SHAPED ACCELERATING CAVITIES *

P. ARCIONI, M. BRESSAN, L. PERREGRINI
Dept. of Electronics, University of Pavia
Via Abbiategrasso 209, 27100 PAVIA, ITALY.

Abstract

We present a new algorithm well suited for the modal analysis of arbitrarily shaped cavities filled with a lossless, isotropic and homogeneous medium. The electric-wall condition is enforced on the field produced by an unknown current sheet, distributed over the cavity wall, and the resulting Electric Field Integral Equation (EFIE) is solved using the method of the moments (MM). Thanks to the special form of the kernel of the EFIE, the algebraic problem can be rearranged to yield the resonating frequencies and the associated currents as eigenvalues and eigenvectors of a standard linear eigenvalue problem. The algorithm yields all resonances up to the maximum frequency of interest by a single evaluation of the MM matrices. For this reason CPU times are reasonably short, even in finding many resonances of quite complicated cavities. The cavity shape is modelled using triangular patches and the code is interfaced with a commercial mechanical CAD.

1. INTRODUCTION

The availability of accurate and efficient computer codes to determine the resonances of arbitrarily shaped cavities is of great importance in the design of interaction structures for particle accelerators. Commercial codes for 3-D structures (MAFIA, ARGUS, etc.) are usually based on Finite Element or Finite Difference methods, which make them very flexible. They need, however, a 3-D mesh and, consequently, a very large number of variables to discretize the problem, thus requiring a large memory allocation and long computing times. When the medium inside the cavity is homogeneous, as in the case of accelerating structures operating in vacuum, it may be advantageous to use a Boundary Integral Method (BIM), that involves quantities defined only on the cavity wall. In this case, indeed, a surface mesh is sufficient, and the order of the matrices involved in the problem reduces dramatically. The conventional approach consists in enforcing the electric-wall condition on the electric field (or on the magnetic field) produced inside the cavity volume V by an unknown current sheet **J** distributed on its boundary S and radiating in free space at an unknown frequency ω. The resulting Electric Field Integral Equation (EFIE) or Magnetic Field Integral Equation (MFIE) is transformed into a complex matrix problem using the method of the moments: the resonating frequencies ω_r are obtained as those particular values of ω that permit the problem to have a non-trivial solution. This solution yields the modal current distribution $\mathbf{J}_r$, from which the modal fields can be calculated. In both cases the coefficients of the MM matrix depend on the frequency through complex transcendental functions, and each resonance must be found through an iterative procedure that require the repeated evaluation of the MM matrix at closely spaced frequencies [1,2]: this may lead to overlong computing times when many resonances are to be found, a drawback that may overwhelm the intrinsic advantage of using the BIM.

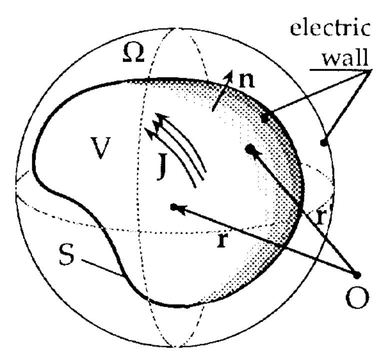

Fig. 1

To overcome this drawback we follow a somewhat different approach, that constitutes the 3-D extension of an algorithm developed for the modal analysis of arbitrarily shaped waveguides [3]. We consider the unknown current **J** radiating, rather than in free space, inside a spherical volume Ω including V and bounded by an electric wall (see Fig. 1). This is possible because, when **J** corresponds to one of the $\mathbf{J}_r$, the field outside V is zero, and therefore it does no matter what boundary condition we impose on the exterior field. As shown in [4], the electric field inside Ω due to the current sheet **J** can be expressed as the sum of two quasi-static contributions plus a high frequency correction:

$$\mathbf{E}(\mathbf{r}) \approx -\nabla \int_{S'} g(\mathbf{r},\mathbf{r}') \frac{\sigma(\mathbf{r}')}{\varepsilon} dS' - j\eta k \int_{S'} \underline{\underline{\mathbf{G}}}(\mathbf{r},\mathbf{r}') \cdot \mathbf{J}(\mathbf{r}')\, dS' - j\eta k^3 \sum_{m=1}^{M} \frac{\mathbf{e}_m(\mathbf{r})}{k_m^2 (k_m^2-k^2)} \int_{S'} \mathbf{e}_m(\mathbf{r}')\cdot \mathbf{J}(\mathbf{r}')\, dS' \qquad (1)$$

where $k=\omega\sqrt{\varepsilon\mu}$, $\eta=\sqrt{\mu/\varepsilon}$, σ is the surface charge density (related to **J** by the continuity condition) and $g(\mathbf{r},\mathbf{r}')$, $\underline{\underline{\mathbf{G}}}(\mathbf{r},\mathbf{r}')$, $\mathbf{e}_m(\mathbf{r}')$ are real frequency independent functions, known in closed form [4]. In particular, $g(\mathbf{r},\mathbf{r}')$ is the electrostatic potential Green's function of the spherical cavity and $\mathbf{e}_m(\mathbf{r}')$, k_m are the (normalized) electric field vector and the corresponding wavenumber of the m-th mode of the spherical resonator. The summation includes all the modes having $k_m \leq k_M$, and it is an accurate approximation of an infinite series, up to a frequency corresponding to about $k_M/2$.

Though more complicated than the equivalent expression for a current radiating in free-space, eq. (1) is much more convenient for the numerical solution of the EFIE, since it is a rational function of k. In fact, thank to this feature the discretization of the EFIE results into a linear matrix eigenvalue problem, as we are going to show in the following.

2. THE ALGORITHM

The surface S is discretized using triangular patches and the unknown functions $\mathbf{J}(\mathbf{r})$ and $\sigma(\mathbf{r})$ are expanded as:

$$\mathbf{J}(\mathbf{r}) \approx \sum_{i=1}^{N} a_i\, \mathbf{f}_i(\mathbf{r}) \quad ; \quad \sigma(\mathbf{r}) \approx -\frac{1}{j\omega} \sum_{i=1}^{N} a_i\, \nabla_S \cdot \mathbf{f}_i(\mathbf{r}) \qquad (2)$$

where $\{\mathbf{f}_i(\mathbf{r})\}$ are the vector subsectional base functions introduced in [5]. Each $\mathbf{f}_i(\mathbf{r})$ has a support Σ_i constituted by the two triangles sharing the i-th edge (see Fig. 2) and is represented by:

(*) Work partially supported by C.N.R. under Contract No. 92.02857.CT07.

$$\mathbf{f}_i(\mathbf{r}) = \begin{cases} (l_i/2A_i^+)\ \rho_i^+ & \text{if } \mathbf{r} \text{ belongs to } T_i^+ \\ -(l_i/2A_i^-)\ \rho_i^- & \text{if } \mathbf{r} \text{ belongs to } T_i^- \\ 0 & \text{elsewhere} \end{cases} \tag{3}$$

where l_i is the length of the i-th edge, A_i^+ and A_i^- denote the area of the two adjacent triangles T_i^+ and T_i^-, and ρ_i^+ and ρ_i^- are vectors emerging from the two vertexes opposite to the i-th edge. The number N of the base function equals the number of the edges. Using these base functions, $\mathbf{J}(\mathbf{r})$ and $\sigma(\mathbf{r})$ are represented by well-behaved functions: in fact, as discussed in [5], the component of the current normal to any edge is continuos, a fact that prevents the need of considering line charges. Moreover, the surface charge density is represented by a zero mean, piece-wise constant function, since we have:

$$\nabla_s \cdot \mathbf{f}_i(\mathbf{r}) = \begin{cases} l_i/A_i^+ & \text{if } \mathbf{r} \text{ belongs to } T_i^+ \\ -l_i/A_i^- & \text{if } \mathbf{r} \text{ belongs to } T_i^- \\ 0 & \text{elsewhere} \end{cases} \tag{4}$$

Introducing eq. (2) into (1), enforcing the boundary condition $\mathbf{n} \times \mathbf{E}(\mathbf{r}) = 0$ ($\mathbf{r} \in S$) and solving the resulting EFIE by the MM by using $\{\mathbf{n} \times \mathbf{f}_i(\mathbf{r})\}$ as test functions, the following set of equations is obtained:

$$\frac{1}{k^2}\sum_{j=1}^{N} C_{ij}\, a_j + \sum_{j=1}^{N} L_{ij}\, a_j + \sum_{m=1}^{M} R_{im}\, b_m = 0 \quad i=1,\dots,N \tag{5}$$

In deriving (5) the set of the M auxiliary variables $\{b_m\}$ have been introduced, which are related to $\{a_i\}$ by the following set of equations:

$$b_m = \frac{k_m^2 k^2}{k_m^2 - k^2}\sum_{j=1}^{N} R_{jm}\, a_j \qquad m=1,\dots,M \tag{6}$$

The other quantities in (5) are defined as:

$$C_{ij} = \int_{\Sigma i}\int_{\Sigma j} \nabla_s \cdot \mathbf{f}_i(\mathbf{r})\, g(\mathbf{r},\mathbf{r}')\, \nabla_s' \cdot \mathbf{f}_j(\mathbf{r}')\ )\ dS'dS \tag{7a}$$

$$L_{ij} = \int_{\Sigma i}\int_{\Sigma j} \mathbf{f}_i(\mathbf{r}) \cdot \underline{\mathbf{G}}(\mathbf{r},\mathbf{r}') \cdot \mathbf{f}_j(\mathbf{r}')\ dS'dS \tag{7b}$$

$$R_{im} = \frac{1}{k_m^2}\int_{\Sigma i} \mathbf{f}_i(\mathbf{r}) \cdot \mathbf{e}_m(\mathbf{r})\ dS \tag{7c}$$

Note that $C_{ij} = C_{ji}$ and $L_{ij} = L_{ji}$ due to the reciprocity properties of g and $\underline{\mathbf{G}}$ [4].

Introducing the vectors $a=\{a_i\}$, $a=\{b_m\}$ and the matrices C, L, R and $D = \mathrm{diag}\{k_m^{-2}\}$, the two sets of equations (5) and (6) can be grouped as follows:

$$\begin{bmatrix} D & \tilde{R} \\ R & L \end{bmatrix}\begin{bmatrix} b \\ a \end{bmatrix} - \frac{1}{k^2}\begin{bmatrix} I & O \\ O & C \end{bmatrix}\begin{bmatrix} b \\ a \end{bmatrix} = 0 \tag{8}$$

where ~ denotes the transpose and I and O are the identity and the zero matrices. Note that all the coefficients of the matrices are independent of the frequency, so that (8) constitutes a generalized linear matrix eigenvalue system in standard form. Moreover, the system matrices are real and symmetric. The largest eigenvalues of (8) yield the first resonating frequencies: they can be found using very efficient library routines.

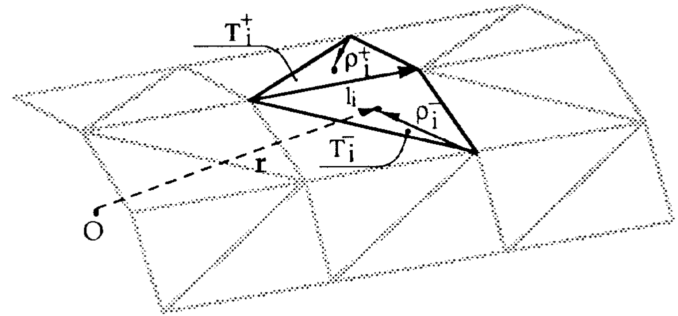

Fig. 2

Compared to the standard EFIE approach [2], a longer time is needed to calculate the MM matrices, due to the more complicated expressions of their coefficients; moreover, besides the desired resonances, this algorithm yields also the resonances of the exterior region Ω–V, i.e. of the fictitious resonator bounded by the spherical surface and the surface S (these spurious solution are easily detected and rejected, since they give rise to a zero field inside the volume V). In spite of these drawbacks, the computer code that implements the new algorithm is very efficient when many resonances are to be calculated. We found that, in the case of typical cavities, the time for computing *all* resonances up to twice the frequency of the fundamental mode is shorter than that needed to find *only one* resonance following the standard EFIE approach (note that, in the conventional approach, typically more than 10 evaluations of the matrices are needed to localize a resonance). Moreover, no problems arise in case of degenerate or nearly degenerate modes.

3. The Computer Code

The algorithm has been implemented in a computer code running under VAX-VMS. The program reads the geometry of the cavity from a formatted file: an interface to a commercial mechanical CAD (PATRAN) is available, that eases the definition of the geometry and the generation of a suitable mesh. It is possible to take advantage of symmetries respect to the coordinate planes to reduce the dimension of the problem. Then coefficients (7) are calculated: since functions $g(\mathbf{r},\mathbf{r}')$ and $\underline{\mathbf{G}}(\mathbf{r},\mathbf{r}')$ diverges when $\mathbf{r} \to \mathbf{r}'$, coefficients c_{ij} and l_{ij} are evaluated analytically in cases where Σ_i and Σ_j overlap (partially or totally). In all other cases a fast gaussian quadrature scheme is used. Problem (8) is solved using the EISPACK routines [6], after a rearrangement, not reported for brevity, useful to reduce memory allocation by taking advantage of the special form of the matrices involved. At present, the selection of the resonances of the outer region must be performed manually, but an automatic procedure for detecting and purging these spurious solution is being implemented. The eigenvalues and the corresponding eigenvectors are stored in a file: a post-processing program can use these data to calculate the normalized modal fields and to evaluate Q-factors and shunt-impedances.

Many calculations have been performed on trirectangular, spherical and cylindrical cavities, and the numerical results have been checked against theoretical ones, in order to validate the program and to investigate the influence of different mesh sizes. Tab. I summarizes the results for a cylindrical cavity (radius=24 cm, heigth=22 cm) analyzed up to about three times the frequency of its fundamental mode using two different mesh size (see Fig. 3a,b). The symmetry respect to the three coordinate planes were exploited and, to minimize the error arising from the discretization of the surface, the volume of the analyzed structures was kept equal to that of the original cavity in both cases.

Using the finest mesh, consisting of 54 triangles (over which 89 base functions were defined), the accuracy is very good for all modes. Even with the coarse mesh (15 triangles, 27 base functions) the accuracy is reasonable for the first few modes, whereas only a rough estimate of the resonating frequency is obtained for the higher modes, as expected. The same table reports, for each mode, the ratio L_m/λ_r of the mean length of the edges to the free-space resonating wavelength. It is noted that accuracies better than 0.3% are obtained for $L_m < \lambda_r/4$. This result, confirmed by the other tests, suggests a rule of thumb for choosing the mesh size. CPU times (on a VAXStation 4000/60) are about 20 s (coarse mesh) and 240 s (fine mesh) for finding all the modes belonging to each class of symmetry. When dealing with symmetries, some intermediate results, not depending on the particular class of symmetry, can be stored and reused for finding modes with different symmetries. This possibility, not yet implemented, will greatly reduce CPU times for the complete analysis.

A second test example refers to the axisymmetric cavity of Fig. 4. One eighth of the surface is modelled using 136 patches (corresponding to 219 base functions). CPU times were 26 minutes for each symmetry class to find the 34 modes up to 10 GHz. In Tab. II the resonating frequencies of the first 20 modes (classified according to their even or odd symmetry respect to the coordinate planes) are compared with measured values and, when possible, with the results obtained by the program SUPERFISH. Fig. 4 shows the electric field of the dominant mode.

ACKNOWLEDGEMENT - The authors wish to thank Prof. G. Conciauro for the fruitful discussions.

REFERENCES

1] F.P. Adams, M.S. de Jong: "A Boundary-Integral-Method Code for Cavity RF Mode Analysis"; Proc. of the 1993 Computational Accelerator Physics Conference, Feb. 22-26, 1993.

2] B.E. Spielman, R.F. Harrington: "Waveguide of Arbitrary Cross Section by the Solution of a Non-Linear Eigenvalue Equation", IEEE Trans. on Microwave Theory and Tech., Vol. MTT-20, no. 9, pp. 578-585, Sept. 1972.

		Coarse Mesh			Fine Mesh		
Mode	theoretical freq. (MHz)	computed frequency	Δ (%)	$\frac{Lm}{\lambda_r}$	computed frequency	Δ (%)	$\frac{Lm}{\lambda_r}$
TM 010	478.42	479.38	0.20	0.20	478.52	0.02	0.10
TM 110	762.29	763.09	0.10	0.31	762.64	0.05	0.16
TE 111	773.98	768.79	-0.67	0.32	774.28	0.03	0.17
TM 011	832.93	827.24	-0.68	0.34	833.28	0.04	0.18
TE 211	913.28	902.24	-1.20	0.38	913.35	0.01	0.20
TM 210	1021.7	1016.7	-0.50	0.42	1022.4	0.07	0.22
TM 111	1022.7	1015.5	0.70	0.42	1024.3	0.15	0.22
TE 011	1022.7	1005.6	-1.70	0.42	1021.9	-0.08	0.22
TE 311	1078.6	1063.7	-1.40	0.44	1079.3	0.06	0.23
TM 020	1098.2	1100.8	0.23	0.45	1101.6	0.30	0.24
TM 211	1228.3	1201.4	-2.20	0.51	1229.0	0.06	0.26
TE 411	1258.6	1237.4	-1.70	0.52	1258.8	0.01	0.27
TE 121	1260.9	1223.3	-3.00	0.52	1259.2	-0.13	0.27
TM 310	1269.3	1236.0	-2.60	0.52	1270.1	0.06	0.27
TM 021	1292.6	1248.8	-3.40	0.53	1298.1	0.40	0.28
TM 120	1395.7	1359.7	-2.60	0.57	1399.2	0.25	0.30
TE 112	1412.0	1398.9	-0.90	0.58	1417.5	0.39	0.30
TM 311	1440.8	1402.1	-2.70	0.59	1445.8	0.35	0.31
TM 012	1445.1	1416.9	-1.90	0.59	1450.0	0.34	0.31
TE 511	1447.0	1429.9	-1.20	0.60	1450.0	0.20	0.31
TE 212	1492.9	1481.5	-0.76	0.61	1498.0	0.34	0.32
TE 221	1498.3	1472.2	-1.70	0.62	1495.6	-0.18	0.32

TAB. I - Resonating frequencies of the cylindrical cavity of Fig. 3

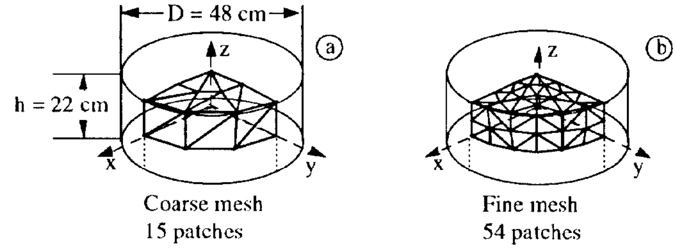

Fig. 3

3] M. Bressan, G. Conciauro, C. Zuffada: "Waveguide Modes Via an Integral Equation Leading to a Linear Matrix Eigenvalue Problem"; IEEE Trans. on Microwave Theory and Tech., Vol. MTT-32, n. 11, Nov. 1984, pp. 1495-1504.

4] M. Bressan, G. Conciauro: "Singularity extraction from the electric Green's function for a spherical resonator"; IEEE Trans. on Microwave Theory and Tech., vol. MTT-33, n. 5, May 1985, pp. 407-414.

5] S. M. Rao, D. R. Wilton, A.W. Glisson: "Electromagnetic Scattering by Surfaces of Arbitrary Shape", IEEE Trans. on Antennas and Propagation, Vol. AP-30, n. 3, May 1982, pp. 409-418.

6] B.S. Garbow, J.M. Boyle, J.J. Dougarde, C.B. Moler: "Matrix eigensystem routines - EISPACK Guide Extension"; in Lecture Notes in Computer Science, no. 51, G. Goos and J. Hartmanis, Eds., Springer-Verlag, 1977.

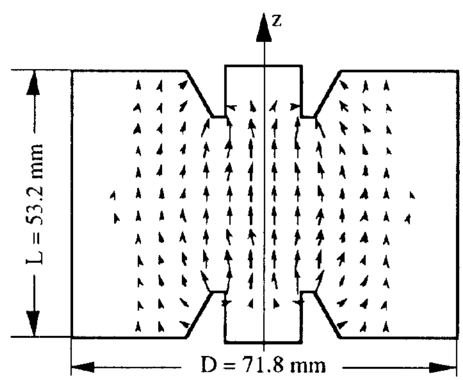

Fg. 4

Symmetry x y z	Calc. res. freq. [GHz]	Superfish	Measured
e e o	2.8642	2.8429	2.8467
e e e	3.9191	3.8976	3.8950
e o e	3.9547	--	3.9357
e e e	5.0429	--	5.0171
e o o	5.0927	--	5.0544
o o e	6.0471	--	6.0208
e o e	6.1687	--	6.1238
e o e	6.3336	--	6.2938
e e o	6.4608	6.4378	6.4150
e o o	6.5880	--	6.5453
e e o	6.9123	--	6.8627
e e o	7.1340	7.0876	7.0874
e e o	7.2389	--	7.1933
e e e	7.5324	7.4741	7.4820
o o e	7.6879	--	7.6327
e e e	7.7238	--	7.6645
e o e	7.7759	--	7.7292
e o o	8.1312	--	8.0604
o o o	8.1327	--	8.1016
e o o	8.3276	--	8.2787

TAB. II - Resonating frequencies of the nose-cone cavity of Fig. 4